

MR ANGIOGRAPHY, FLOW, AND ENDOTHELIAL FUNCTION

A novel method for assessing arterial endothelial function using phase contrast magnetic resonance imaging: vasoconstriction during reduced shear

HARRY A. SILBER, M.D., PH.D.,^{1,*} PAMELA OUYANG, M.D.,¹ DAVID A. BLUEMKE, M.D., PH.D.,² SANDEEP N. GUPTA, PH.D.,³ THOMAS K. FOO, PH.D.,³ and JOAO A. C. LIMA, M.D.^{1,2}

¹*Division of Cardiology, Department of Medicine, Johns Hopkins University, School of Medicine, Baltimore, Maryland, USA*

²*Department of Radiology, Johns Hopkins University, School of Medicine, Baltimore, Maryland, USA*

³*Applied Science Laboratory, General Electric Healthcare Technologies, Milwaukee, Wisconsin, USA*

We investigated whether endothelial-dependent arterial constriction during reduced shear can be measured using phase contrast magnetic resonance imaging (PCMRI). A cross-section of the femoral artery was acquired during a 5-minute distal occlusion in 33 subjects. Systolic shear rate and radius were measured from the velocity profile via a best-fit parabola. Systolic shear rate decreased immediately after cuff inflation (404 ± 78 to 233 ± 75 sec^{-1} $p < .0001$). Radius decreased at 2 min into inflation ($3.52 \pm .41$ to $3.43 \pm .42$ mm, $p < .0001$). In conclusion, arterial constriction during reduced flow can be measured using PCMRI. This new method may add important information toward a comprehensive evaluation of endothelial function.

Key Words: Endothelial function; Vasoconstriction; Magnetic resonance imaging; Blood flow

1. Introduction

Vascular endothelium, the inner lining of blood vessels, is crucially important to maintaining vascular health. Endothelial cells regulate thrombosis, inflammation, vasomotion, and cell proliferation through the synthesis and release of substances including nitric oxide and endothelin-1 (1). Cardiovascular risk factors are associated with endothelial dysfunction (2–4), and agents that reduce cardiovascular risk also improve endothelial function (5). Hence, endothelial dysfunction is considered to be an important common pathway by which risk factors promote atherosclerosis (6). Furthermore, endothelial dysfunction is associated with coronary events (7). Consequently, there is much interest in assessing endothelial function noninvasively (6, 8, 9).

The most common method of assessing endothelial function noninvasively uses ultrasound to measure a change in arterial size after the induction of transient hyperemia (2, 10, 11). This method exploits the fact that shear stress is the primary hemodynamic stimulus of endothelial function (12) and that

increased shear stress induces dilation in human peripheral arteries (2, 10, 11) due primarily to nitric oxide release (13). Conversely, with hyperemia-induced dilation, decreased flow induces constriction of peripheral arteries (2, 11, 14). Low-flow mediated constriction is also endothelial-dependent and is mediated by endothelin-1 via endothelin A receptors (15). The actions of endothelin-1 generally oppose the vasoprotective effects of nitric oxide, which is the predominant endothelially released substance responsible for hyperemia-induced dilation (16). Therefore, studying low-flow mediated constriction in addition to hyperemia-induced dilation may allow a more comprehensive assessment of endothelial function. However, low-flow mediated constriction has been studied much less extensively than flow mediated dilation. Furthermore, the relationship between the stimulus of shear reduction and the response of vasoconstriction has not been determined. This relationship may add further useful information in the noninvasive evaluation of endothelial function. We have previously used phase contrast magnetic resonance imaging (PCMRI) to determine the relationship between flow mediated dilation and the hyperemic shear stimulus for flow mediated dilation (17, 18). Magnetic resonance imaging (MRI) offers important advantages over ultrasound in assessing endothelial function: MRI is not as critically operator-dependent, it obtains a cross-sectional image, and it allows the simultaneous measurement of shear rate, the stimulus for flow-mediated vasoactivity. In this study, we hypothesized that

Received 16 September 2004; accepted 19 April 2005.

*Address correspondence to Harry A. Silber, M.D., Ph.D., Cardiology A-1 East, Johns Hopkins Bayview Medical Center, 4940 Eastern Ave., Baltimore, MD 21224, USA; Fax: (410) 550-1183; E-mail: hsilber@jhmi.edu

PCMRI could also be used to measure shear rate changes and resulting constriction during reduced flow in the peripheral arteries. Further, we investigated the relationship between the acute shear rate reduction at the onset of low-flow and the resulting degree of arterial constriction.

2. Methods

2.1. Subjects

Thirty-three healthy subjects (16 men and 17 women), ages 20–41, with no cardiovascular risk factors, including hypertension, diabetes, hyperlipidemia, smoking, obesity or cardiac disease in a first-degree relative, were studied. No subject was acutely ill or was on any vasoactive medication. The study protocol was approved by the Institutional Review Board at the Johns Hopkins School of Medicine. All subjects gave written informed consent.

2.2. Study protocol

Subjects abstained from eating or drinking anything except water for at least 6 hours before the study. Baseline blood pressure was recorded. PCMRI was performed using a 1.5T scanner (CV/i, General Electric Medical Systems, Milwaukee, WI) equipped with cardiac gradient coils (40 mT/m, 120 T/m/s). Electrocardiographic leads were placed on the thorax. A dual cardiac phased array receiving coil was placed anterior and posterior to the upper thigh. A sphygmomanometer cuff was placed on the lower thigh. Phase-contrast images were obtained at baseline. The cuff was then inflated at least 20 mmHg above the subject's measured systolic blood pressure for 5 minutes, which is the standard cuff inflation time in flow mediated dilation studies. This standard duration was used to maximize the scanning time during cuff inflation and thus maximize signal-to-noise ratio during reduced flow. The inflated cuff totally occludes blood flow through the distal femoral artery, but some flow remains in the proximal femoral artery being imaged. This is due to branches originating from the femoral artery between the proximal cross-section being imaged and the distal section being occluded. These branches supply muscle and skin to the proximal thigh. Images using the same fixed cross-sectional axial prescription as at the baseline were obtained immediately after onset of cuff inflation and at two minutes into cuff inflation. Scanning during low flow was begun at 2 minutes into cuff inflation because of a previous study suggesting that the arterial dimension reaches steady state at approximately 2 minutes into distal occlusion (19). Serum values of glucose, hematocrit, and fasting lipid panel were obtained after the scanning portion of the study. To assess the reproducibility of measurements, the study was repeated in each of eight subjects during a second session.

2.3. Imaging protocol

Coronal and axial scout images were obtained to locate the superficial femoral artery and to verify that the artery was

parallel to the magnet bore. Axial scout images were used to locate a plane approximately 3 to 5 mm distal to where the common femoral artery bifurcates into the superficial and deep femoral arteries. Phase contrast scans were gated to the electrocardiogram signal. A single axial imaging plane was prescribed in order to image the arterial cross-section. The imaging parameters were: Matrix size 256×128 , field-of-view 10 by 10 cm, slice thickness 3 mm, flip angle 25 degrees, bandwidth 31.2 kHz, repetition time (TR) 11.43 msec, echo time (TE) 5.25 msec, 8 views per segment, first order flow compensation, no phase-wrap, and no magnitude weighting. Also, settings of 16 number of excitations (NEX) and maximum encoded velocity value (VENC) 60 cm/sec 2 NEX and VENC 50 cm/sec immediately after onset of cuff inflation, and 8 NEX and VENC 50 cm/sec at two minutes into cuff inflation were used at baseline. The use of 8 NEX during cuff inflation increased scan time to approximately 2 minutes but resulted in an increased signal-to-noise ratio. Resulting temporal resolution for all scans was about 180 msec.

2.4. Data analysis

Image data was imported via Scion Image (Scion Corporation, Frederick, MD) into a spreadsheet-based (Excel, Microsoft Corporation, Mountain View, CA) program created in our laboratory. The cardiac phase closest to peak systole was used for measuring radius, shear, and flow. Peak systole was identified by choosing the image with the greatest peak velocity. An approach modified from one by Oyre et al. (20) was used to calculate shear and radius. In our approach, the limits of the arterial diameter were estimated in two orthogonal axes. An initial estimate of the center of the cross-section was calculated from those limits. The cross-section was divided into 12 sectors around the estimated center. For each sector, outer radius of the velocity profile was estimated. A ring segment of datapoints with radius ranging from slightly less than the initially estimated outer radius to about 1 mm inward toward the estimated center was used. The velocity pixels in the ring segment of the sector were fit by least-squares method to a parabola with the assumption that blood flow velocity at the lumen wall is zero. Shear rate was calculated as the slope of the velocity profile at the lumen-wall interface. Radius was calculated as the distance from the center of the velocity parabola to the point where the parabola crosses zero velocity. The calculated lumen radius and shear values were averaged over the 12 sectors in the arterial cross-section. This approach provides sub-pixel precision in calculating lumen radius and was shown to be accurate when compared to glass tubes of known manufactured diameter (20). Furthermore, the approach is not constrained by the geometry of the lumen perimeter, i.e. the arterial cross-section does not have to be perfectly circular. Systolic flow was measured directly by summing all of the velocity pixels in the arterial cross-section. Shear rate immediately after cuff inflation was calculated using flow measured at two minutes

Table 1. Subject characteristics and measurements

Characteristic	Value
n	33 (17F/16M)
Age [years]	27 ± 5
BMI [kg/m ²]	23 ± 3
TChol [mg/dL]	172 ± 31
HDL [mg/dL]	61 ± 13
Trig [mg/dL]	83 ± 32
LDL [mg/dL]	94 ± 27
Glucose [mg/dL]	81 ± 9
Hematocrit [%]	42 ± 3
Shear rate, baseline [sec ⁻¹]	404 ± 78
Shear rate at 0' into CI [sec ⁻¹]	233 ± 75*
Shear rate at 2' into CI [sec ⁻¹]	252 ± 75* [†]
Radius, baseline [mm]	3.52 ± .41
Radius at 2' into CI [mm]	3.43 ± .42*
Percent change in radius	-2.8 ± 2.5

Values represent mean ± SD. F = females; M = males; BMI = body mass index; Tchol = total cholesterol; HDL = high-density lipoprotein; Trig = triglycerides; LDL = low-density lipoprotein; C.I. = cuff inflation.

*p < .0001 vs. baseline.

[†]p < .0001 vs. 0' into cuff inflation.

into cuff inflation and using radius measured at baseline, using the Poiseuille equation:

$$\text{shear rate} = 4k(\text{flow})/(\pi)(\text{radius}^3) \quad (1)$$

The constant k is necessary because the velocity profile during systole is slightly blunted rather than being a fully developed parabola (17–22). Consequently, the true shear rate is greater than what would be calculated using a fully developed parabolic velocity profile. Thus k describes how many times greater the shear rate is than would be predicted by a fully developed paraboloid given the same radius and flow. The value of k was determined for each subject by directly measuring radius, flow, and shear rate at baseline and at 2-minutes into cuff inflation. The value of the k was solved for:

$$k = (\text{shear rate})(\pi)(\text{radius}^3)/([4][\text{flow}]) \quad (2)$$

The value of k at 2 minutes into cuff inflation was used in the calculation of shear rate immediately after cuff inflation. Degree of vasoconstriction was expressed as the percent change in radius from baseline to two minutes into cuff inflation.

2.5. Statistical analysis

Results are expressed as mean value ± SD. A paired t-test was used to compare measured parameters before and during cuff inflation. Linear regression analysis was used to assess the relationships between variables. A P value less than 0.05 was considered significant. To assess reproducibility of radius, shear rate, and percent constriction measurements in

the eight subjects who underwent repeat scans within-subject standard deviation was calculated.

3. Results

Subject characteristics and measurements are shown in Table 1. Figure 1 shows phase contrast images of a typical femoral artery at baseline and at two minutes into cuff inflation. Following each image is a surface plot of the velocity profile and a plot of velocity versus radius for one of 12 sectors around the arterial circumference. Shear rate decreased from 404 ± 78 sec⁻¹ at baseline to 233 ± 75 sec⁻¹ immediately after cuff inflation (p < .0001), then recovered partially to 252 ± 75 sec⁻¹ at two minutes into cuff inflation (p < .0001, Fig. 2). Arterial radius decreased from 3.52 ± .41 mm at baseline to 3.43 ± .42 mm at two minutes into cuff inflation (p < .0001). The average percent change in radius from baseline to two minutes into cuff inflation was -2.8 ± 2.5%. The percent change in radius from baseline to two minutes into cuff inflation was proportional to the percent change in shear rate from baseline to immediately after cuff inflation (r = 0.36, p = .028, Fig. 3). Also, the absolute change in radius from baseline to two minutes into cuff inflation was proportional to the percent change in shear rate from baseline to immediately after cuff inflation (r = 0.44, p = 0.0097). The percent change

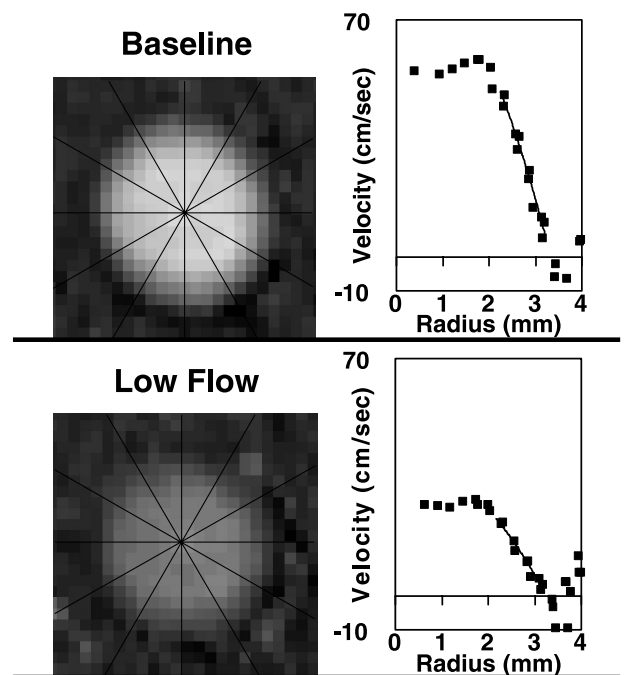


Figure 1. For a typical femoral artery, a velocity-encoded phase contrast magnetic resonance image of the cross-section during systole is shown at baseline and at two minutes into cuff inflation (low flow). Superimposed on each image are the 12 sectors into which the data points are divided for analysis. Each phase image is followed by a plot of systolic velocity versus radius for one of 12 sectors.

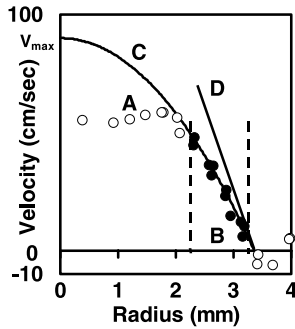


Figure 2. Steps taken to determine radius and shear rate in one of the sectors at baseline for a typical femoral artery. The method of analysis is adapted from Oyre et al. (20). A. Radial plot of velocity datapoints. B. The datapoints in a 1-mm wide range (darkened circles) near the arterial wall are used to find the best-fit parabola. C. Best fit parabola: The equation for velocity (V) as a function of r , the distance from the center, is $V(r) = V_{max} (1 - [r^2/R^2])$. Radius (R) of the artery is where the value of the best-fit parabola $V(r)$ equals 0, which is at the vessel wall. D. Shear rate = absolute value of the slope of the parabola at the arterial wall where $r = R$: $ABS (dV[r]/dr) = 2V_{max}/R$.

in shear rate from baseline to immediately after cuff inflation was inversely related to baseline arterial size ($r = 0.42$, $p = 0.015$). The ratio of percent change in radius divided by the percent change in shear rate was greater for women than for men ($.091 \pm .072$ vs. $.054 \pm .054$, $p = .049$). However, this ratio was inversely related to baseline radius ($p = .040$, $r = 0.39$, Fig. 4), and baseline radius was smaller in women than in men ($3.29 \pm .33$ mm vs. $3.78 \pm .34$ mm, $p = .0001$). The constant k in the Poiseuille relationship was slightly greater at two minutes into cuff inflation than at baseline, 1.14 ± 0.08 vs. 1.18 ± 0.12 ($p = .035$), suggesting that the velocity profile was slightly more blunted during cuff

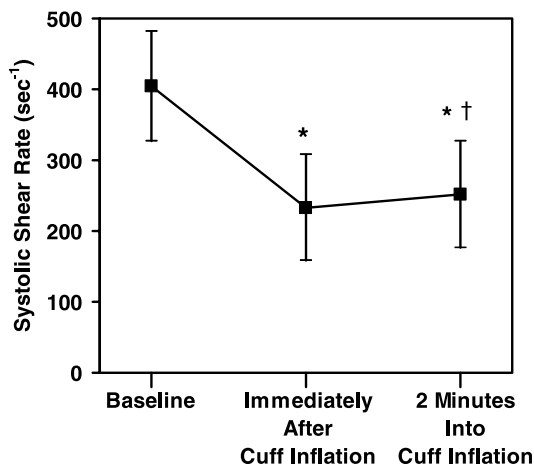


Figure 3. Time-course of systolic shear rate in the femoral artery at baseline immediately after cuff inflation and at two minutes into cuff inflation. * $P < .0001$ vs. baseline, † $P < .0001$ vs. immediately after cuff inflation.

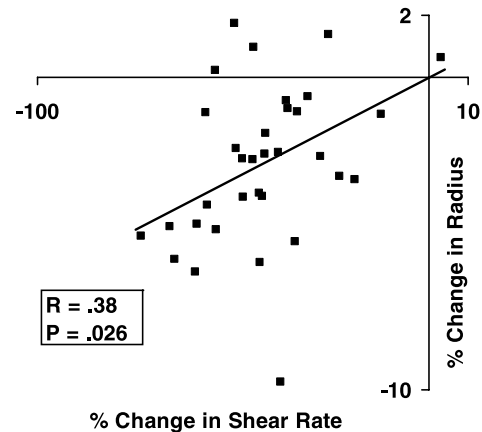


Figure 4. Percent reduction in radius at two minutes into cuff inflation is proportional to the percent reduction in shear rate at the onset of cuff inflation.

inflation. For scans repeated on a second occasion, the average time between sessions was 125 ± 66 days (range 48–255 days). The repeated measurement, within-subject standard deviation of baseline radius was 0.13 mm; radius at 2 minutes into cuff inflation, 0.14 mm; baseline shear rate, 35 sec^{-1} ; shear rate immediately after onset of cuff inflation, 35 sec^{-1} . The repeated measurement, within-subject standard deviation of percent change in radius was 1.6%.

4. Discussion

The major findings of this study are: 1) The reduction in shear rate during low-flow in peripheral arteries and the resulting decrease in radius can be measured using PCMRI and 2) The percent decrease in radius is proportional to the percent reduction in shear rate. The stimulus-response relationship in low-flow mediated vasoconstriction may add useful information to the assessment of endothelial function.

Low-flow mediated vasoconstriction in peripheral arteries has been measured using ultrasound but has been studied much less extensively than hyperemia-induced dilation. Vasoconstriction was seen in response to reduced flow in hypercholesterolemic subjects but not in normocholesterolemic controls (23). In fact, the degree of reduction was closely related to the degree of elevation of blood cholesterol and of its low density lipoprotein fraction. Cholesterol lowering therapy reduced the degree of vasoconstriction in hypercholesterolemic subjects (24). Vasoconstriction during reduced flow was detected in smokers but not nonsmokers (25). The stimulus-response relationship in low-flow mediated vasoconstriction may add useful information when assessing whether two different populations may be at different levels of cardiovascular risk. Levenson et al. (19) detected no difference in brachial artery diameter reduction between men and women but did detect a difference when the percent change in

diameter was normalized to the percent change in shear rate. We also found that the normalized ratio was greater in women. However, this may be explained by the smaller arterial size in women, since we also found an inverse correlation between the normalized ratio and arterial size (Fig. 4).

In all, four groups of investigators besides ours have analyzed vasoconstriction during distal occlusion in studies that included subjects without risk factors. All four groups imaged the brachial artery before and during wrist or forearm occlusion. Three of the groups detected a decrease in arterial size (10, 11, 19). One of the three groups detected no constriction in subjects without risk factors in their first study (23), but the same group did detect constriction in such a group in a later paper (19). It is possible that technical advances allowed them to detect the change in the later study. The group that did not detect constriction (25) had differences from our study that may account for the different findings. Besides the different measuring technique (i.e. ultrasound versus MRI), another difference is that the average age of their group was 12 years older than the average age of our group. The effect of age on low-shear mediated vasoconstriction remains to be explored. If low-flow mediated constriction is decreased with age, it may be more difficult to detect.

Hyperemia-induced dilation is predominantly dependent on endothelial nitric oxide release, whereas low-flow mediated constriction is dependent on endothelin-1 release. The anti-atherosclerotic actions of endothelial-derived nitric oxide on promoting vasodilation, inhibiting inflammation, inhibiting platelet aggregation, and inhibiting smooth muscle proliferation are generally opposed by the actions of endothelin-1 (16). Therefore, measuring the stimulus-response relationship in low-flow mediated vasoconstriction may provide additional useful information on the balance between these two mediators of atherosclerosis development. Although low-flow mediated vasoconstriction has been shown to be dependent on endothelin-1, it would also be important to assess its dependence on nitric oxide. This could be tested invasively by infusing arterially a nitric oxide antagonist before occluding the distal limb.

Magnetic resonance imaging has recently been employed to assess arterial endothelial function by measuring flow mediated dilation (17, 18, 26–29) or reactive hyperemia (30). A fixed cross-section can be imaged repeatedly, reducing operator dependence. An additional advantage of using velocity-encoded MRI is that flow velocity information across the entire cross-section is obtained simultaneously with dimension information, enabling calculation of the shear stimulus for vasoactivity (17, 18).

An advantage of evaluating endothelial function during cuff inflation is that a steady state is reached, as opposed to the post-release period when the hyperemia and subsequent dilation are more transient. This allows the scan duration to be longer, which enables an increased signal-to-noise ratio of the image. A recent study suggested that flow and radius do not change significantly between two and five minutes into cuff

inflation (19). Consequently, we designed our scanning protocol to allow for a scan duration of about 2 minutes, starting at two minutes into cuff inflation, thus optimizing signal to noise ratio during the cuff inflation period.

The fact that the constant k in the Poiseuille relationship was slightly greater at two minutes into cuff inflation than at baseline suggests that the velocity profile was slightly more blunted during cuff inflation. This likely reflects the fact that flow decreased to a greater extent than radius did from baseline to two minutes into cuff inflation. A velocity profile is more blunted when arterial radius is large relative to blood flow velocity (31). In this case, the effect, though statistically significant, was very slight in practical terms.

We used the cardiac phase with peak flow to calculate shear rate and radius. In other cardiac phases, the signal-to-noise ratio is much lower and the flow is more complex with regard to spatial distribution in the arterial cross-section. The fact that radius was measured during systole may help to explain why an increase in radius was seen during reduced flow in some cases. Since the occlusion was distal to the imaged cross-section, there may sometimes have been increased systolic distension of the artery proximal to the occlusion. More consistent and pronounced constriction may be measured in future studies if diastolic cardiac phases are used for radius measurements, perhaps based on the magnitude images.

We could not directly measure the shear rate stimulus for constriction instantaneously after distal occlusion because the artery would have accomplished most of its constriction by the end of a 35-second scan. A more rapid scan would have sacrificed signal-to-noise ratio. Instead, we calculated shear rate at onset of occlusion based on the steady state measurement of radius before occlusion, and on the steady state measurement of flow at 2 minutes into occlusion. To validate our approach, we directly measured flow and radius immediately after cuff inflation in a subset of 12 subjects to evaluate whether it differed consistently from flow measured at 2 minutes into cuff occlusion. The duration of the scans started immediately after cuff inflation were approximately 35 seconds. Flow measured during the scans started immediately after cuff inflation was not different from flow measured starting at 2 minutes into cuff inflation [$p = \text{nonsignificant (NS)}$]. However, the radius measured during the scan immediately following cuff inflation was also not different from that measured at 2 minutes into distal occlusion ($p = \text{NS}$). This means that, during the 35 seconds into distal occlusion that it took to image the artery, the radius was already close to its final value. This is important because radius is a very strong determinant of shear rate. Thus, the instantaneous shear rate immediately after cuff inflation cannot be accurately measured using a 35-second scan. These findings justify our approach of calculating instantaneous shear rate at onset of cuff inflation using baseline radius and using flow at 2 minutes into occlusion.

The percent change in shear rate from baseline to immediately after cuff inflation was inversely related to

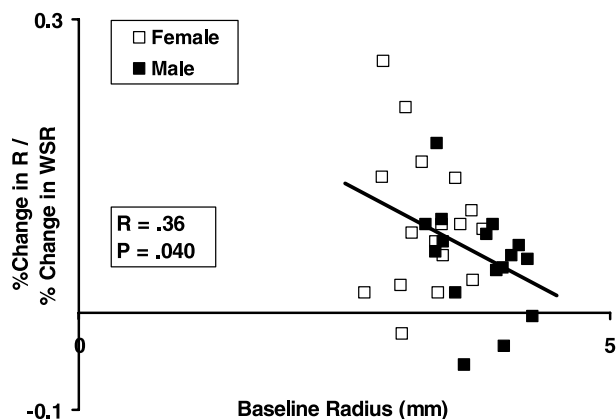


Figure 5. The ratio of percent change in radius (R) to percent change in wall shear rate (WSR) is inversely related to baseline radius. The dependence of the ratio on arterial size may explain why the ratio is greater in women than in men.

baseline arterial size. Therefore, the large range of changes in shear rate was due in part the range of arterial sizes studied. Figure 5 suggests that normalizing the percent change in radius to percent change in shear rate may improve the assessment of endothelial-dependent low-flow mediated constriction. However, this approach needs to be tested in future studies comparing groups with and without endothelial dysfunction.

Although shear-mediated vasoactivity is a mechanism by which the endothelium autoregulates shear stress (1), the degree of constriction during distal occlusion did not restore the shear rate to its baseline value. This likely reflects that the degree of acute shear reduction was well beyond that which might be expected to occur in non-experimental circumstances.

The change in shear rate from immediately after cuff inflation to 2 minutes into cuff inflation was highly significant despite the small change, the large standard deviation, and the small sample size. This is due to the use of a paired *t*-test and to the highly significant change in radius. Since flow is assumed to be the same at 2 minutes into inflation as it is immediately after onset of cuff inflation, it is the decrease in radius that drives the significant increase in shear rate. Since shear rate is proportional to $1/\text{radius}^3$, a small but significant decrease in radius will produce a significant increase in shear rate.

4.1. Limitations

There were several limitations to this study. Accuracy of measurement is limited by the need to optimize the MRI scanning parameters that determine spatial resolution, temporal resolution, signal-to-noise ratio, and duration of image acquisition. For example, increasing temporal resolution typically compromises signal-to-noise ratio and therefore accuracy of radius measurement. We chose parameters to prioritize accurate radius measurement; therefore, the image is not necessarily obtained at the exact point of maximal

instantaneous flow in the cardiac cycle. Another limitation is the small percent change in radius during distal occlusion, especially considering the relatively large within-subject variability. It remains to be determined whether and how low-flow mediated constriction of the femoral artery is different in an older group or a group with cardiovascular risk factors. Such a study will be necessary to determine if this test will be useful in discriminating between groups of people with and without known endothelial dysfunction.

5. Conclusion

During a low-flow state induced in the femoral artery, the reduction in shear rate and the resulting endothelial-dependent arterial constriction can be measured using PCMRI. The arterial constriction response is proportional to the acute reduction in shear rate. The constriction response per shear reduction stimulus is higher in women but may be due to their smaller arterial size. Measuring the stimulus-response relationship in low-flow mediated vasoconstriction using PCMRI may add important information toward a more comprehensive evaluation of endothelial function.

Acknowledgments

This work was supported by grant K23-HL-04477 (H.S.) from the National Heart, Lung, and Blood Institute. The authors gratefully acknowledge the assistance of Ann Munson, M.S., R.D., in coordinating the research participants.

References

1. Busse R, Fleming I. Regulation of endothelium-derived vasoactive autacoid production by hemodynamic forces. *Trends Pharmacol Sci* 2003; 24:24–29.
2. Celermajer DS, Sorensen KE, Gooch VM, Spiegelhalter DJ, Miller OI, Sullivan ID, Lloyd JK, Deanfield JE. Non-invasive detection of endothelial dysfunction in children and adults at risk of atherosclerosis. *Lancet* 1992; 40:1111–1115.
3. Celermajer DS, Sorensen KE, Bull C, Robinson J, Deanfield JE. Endothelium-dependent dilation in the systemic arteries of asymptomatic subjects relates to coronary risk factors and their interaction. *J Am Coll Cardiol* 1994; 24:1468–1474.
4. Lieberman EH, Gerhard MD, Uehata A, Selwyn AP, Ganz P, Yeung AC, Creager MA. Flow-induced vasodilation of the human brachial artery is impaired in patients < 40 years of age with coronary artery disease. *Am J Cardiol* 1996; 78:1210–1214.
5. Vogel RA, Corretti MC, Plotnick GD. Changes in flow-mediated brachial artery vasoactivity with lowering of desirable cholesterol levels in healthy middle-aged men. *Am J Cardiol* 1996; 77:37–40.
6. Widlansky ME, Gokce N, Keaney JF Jr, Vita JA. The clinical implications of endothelial dysfunction. *J Am Coll Cardiol* 2003; 42:1149–1160.
7. Neunteufl T, Heher S, Katzenschlager R, Wolf G, Kostner K, Maurer G, Weidinger F. Late prognostic value of flow-mediated dilation in

- the brachial artery of patients with chest pain. *Am J Cardiol* 2000; 6:207–210.
8. Kuvin JT, Karas RH. Clinical utility of endothelial function testing: ready for prime time? *Circulation* 2003; 107:3243–3247.
 9. Verma S, Buchanan MR, Anderson TJ. Endothelial function testing as a biomarker of vascular disease. *Circulation* 2003; 108:2054–2059.
 10. Anderson EA, Mark AL. Flow-mediated and reflex changes in large peripheral artery tone in humans. *Circulation* 1989; 79:93–100.
 11. Sinoway LI, Hendrickson C, Davidson WR Jr, Prophet S, Zelis R. Characteristics of flow-mediated brachial artery vasodilation in human subjects. *Circ Res* 1989; 64:32–42.
 12. Davies PF, Zilberberg J, Helmke BP. Spatial microstimuli in endothelial mechanosignaling. *Circ Res* 2003; 92:359–370.
 13. Joannides R, Haefeli WE, Linder L, Richard V, Bakkali EH, Thuillez C, Luscher TF. Nitric oxide is responsible for flow-dependent dilatation of human peripheral conduit arteries in vivo. *Circulation* 1995; 91:1314–1319.
 14. Joannides R, Costentin A, Iacob M, Bakkali EH, Richard MO, Thuillez C. Role of arterial smooth muscle tone and geometry in the regulation of peripheral conduit artery mechanics by shear stress. *Clin Exp Pharmacol Physiol* 2001; 28:1025–1031.
 15. Spieker LE, Luscher TF, Noll G. ET_A receptors mediate vasoconstriction of large conduit arteries during reduced flow in humans. *J Cardiovasc Pharmacol* 2003; 42:315–318.
 16. Alonso D, Radomski MW. The nitric oxide-endothelin-1 connection. *Heart Fail Rev* 2003; 8:107–115.
 17. Silber HA, Bluemke DA, Ouyang P, Du YP, Post WS, Lima JA. The relationship between vascular wall shear stress and flow-mediated dilation: endothelial function assessed by phase-contrast magnetic resonance angiography. *J Am Coll Cardiol* 2001; 38:1859–1865.
 18. Silber HA, Ouyang P, Bluemke DA, Gupta SN, Foo TK. Why is flow mediated dilation dependent on arterial size? Assessment of the shear stimulus using phase contrast magnetic resonance imaging. *Am J Physiol* 2005; 288:H822–H828.
 19. Levenson J, Pessana F, Garipey J, Armentano R, Simon A. Gender differences in wall shear-mediated brachial artery vasoconstriction and vasodilation. *J Am Coll Cardiol* 2001; 3:1668–1674.
 20. Oyre S, Ringgaard S, Kozerke S, Paaske WP, Scheidegger MB, Boesiger, Pedersen EM. Quantitation of circumferential subpixel vessel wall position and wall shear stress by multiple sectored three-dimensional paraboloid modeling of velocity encoded cine MR. *Magn Reson Med* 1998; 40:645–655.
 21. Simon AC, Levenson J, Flaud P. Pulsatile flow and oscillating wall shear stress in the brachial artery of normotensive and hypertensive subjects. *Cardiovasc Res* 1990; 24:129–136.
 22. Hoeks AP, Samijo SK, Brands PJ, Reneman RS. Noninvasive determination of shear-rate distribution across the arterial lumen. *Hypertension* 1995; 26:26–33.
 23. Filitti V, Giral P, Simon A, Merli I, Del Pino M, Levenson J. Enhanced constriction of the peripheral large artery in response to acute induction of a low-flow state in human hypercholesterolemia. *Arterioscler Thromb* 1991; 11:161–166.
 24. Megnien JL, Simon A, Andriani A, Segond P, Jeannin S, Levenson J. Cholesterol lowering therapy inhibits the low-flow mediated vasoconstriction of the brachial artery in hypercholesterolaemic subjects. *Br J Clin Pharmacol* 1996; 42:187–193.
 25. Stadler RW, Ibrahim SF, Lees RS. Measurement of the time course of peripheral vasoactivity: results in cigarette smokers. *Atherosclerosis* 1998; 138:197–205.
 26. Alexander MR, Kitzman DW, Khaliq S, Dart SN, Hamilton CA, Herrington DM, Link KM, Hundley WG. Determination of femoral artery endothelial function by phase contrast magnetic resonance imaging. *Am J Cardiol* 2001; 88:1070–1074.
 27. Sorensen MB, Collins P, Ong PJ, Webb CM, Hayward CS, Asbury EA, Gatehouse PD, Elkington AG, Yang GZ, Kubba A, Pennell DJ. Long-term use of contraceptive depot medroxyprogesterone acetate in young women impairs arterial endothelial function assessed by cardiovascular magnetic resonance. *Circulation* 2002; 106:1646–1651.
 28. Tan P, Hamilton CA, Link KM, Kitzman DW, Hundley WG. Automated analysis of phase-contrast magnetic resonance images in the assessment of endothelium-dependent flow-mediated dilation. *J Cardiovasc Magn Reson* 2003; 5:325–332.
 29. Wiesmann F, Petersen SE, Leeson PM, Francis JM, Robson MD, Wang Q, Choudhury R, Channon KM, Neubauer S. Global impairment of brachial, carotid, and aortic vascular function in young smokers: direct quantification by high-resolution magnetic resonance imaging. *J Am Coll Cardiol* 2004; 44:2056–2064.
 30. Mohiaddin RH, Gatehouse D, Moon JC, Youssuffidin M, Yang GZ, Firmin DN, Pennell DJ. Assessment of reactive hyperaemia using real time zonal echo-planar flow imaging. *J Cardiovasc Magn Reson* 2002; 4:283–287.
 31. Nichols WM, O'Rourke MF. McDonald's Blood Flow in Arteries: Theoretical, Experimental and Clinical Principles. 4th ed. New York: Oxford University Press, 1998.